Formation of Lateral Low Density In(Ga)As Quantum Dot Pairs in GaAs Nanoholes

P. Alonso-González, J. Martín-Sánchez, Y. González, B. Alén, D. Fuster, and L. González*

Instituto de Microelectrónica de Madrid (IMM-CNM, CSIC), Isaac Newton, 8 Tres Cantos, Madrid 28760 Spain

ABSTRACT: In this work we present a growth procedure to form lateral In(Ga)As quantum dot pairs by using a low density, 2×10^8 cm^{-2}, GaAs nanohole template previously formed in situ by droplet homoepitaxy. In particular, by changing the arsenic pressure at which InAs is grown on the template, we demonstrate the possibility to select the formation of single quantum dots (QD) or QD pairs inside each of the nanoholes. In the case of QD pairs, the ensemble photoluminescence (PL) as a function of excitation power and temperature reveals spectral signatures typical of laterally coupled nanostructures.

Introduction

The use of semiconductor quantum dots (QD) as active elements in different optoelectronic devices for quantum information technology[1−3] is currently receiving much attention. Triggered sources of single photons[3] or entangled photon pairs[1] have been achieved using these nanostructures as active elements. In addition, by embedding them within a photonic crystal microcavity, quantum phenomena based on strong light-matter coupling are also being studied.[2] In this sense, the ability to obtain a precise control in size, spatial location, and number of nanostructures has become a highly desirable issue.[4−6] In particular, the formation of different distributions of QD in close proximity[7] permits a precise study of coupling and coherence that is strictly necessary for the creation of future functional units in the field of quantum computing and communication.[8] In this way, the growth of vertically stacked self-assembled QD has been deeply studied during the last years allowing the direct observation of controlled coupling in a quantum dot molecule (QDM).[9] For applications, however, the development of a lateral configuration of coupled nanostructures is highly desirable as it would extend the coupling to two dimensions and it would facilitate the gating technology. Experimentally, the lateral coupling of two adjacent QD has been recently demonstrated.[10] In this case, the fabrication method was based on the growth selectivity of QD into previously in situ etched nanoholes.[11] In a simple similar way, droplet epitaxy technique[12,13] has emerged as a straightforward in situ fabrication method to obtain, in a self-assembled way, templates of low density nanoholes on GaAs substrates. In particular, by means of InAs selective growth at these nanoholes, different distributions of nanostructures[14−18] have been fabricated presenting good optical properties at the single nanostructure level.[19] Moreover, by using the appropriate growth conditions during the capping process of these nanostructures, the formation of mounds spatially located over the buried QD has also been demonstrated.[2] This effect permits the localization of the nanostructures at the top surface,[20] making easier any further technological processes for application of these nanostructures into devices.

In this work, we have explored the ability to design the formation of low density In(Ga)As QD pairs (2×10^8 cm^{-2}) by the use of a template of nanoholes in situ formed by droplet homoepitaxy on a GaAs(001) buffer layer. We have observed nucleation of single QD or QD pairs inside each of the nanoholes depending on the arsenic pressure used during InAs deposition. The photoluminescence (PL) emission of the QD pairs, in particular the evolution of the peak energy and full width at half-maximum (fwhm) as a function of excitation intensity and temperature respectively, show signatures of laterally coupled quantum systems[21] as has been previously reported.[22,23]

Experimental Procedure

The samples were grown by molecular beam epitaxy (MBE) and topographically characterized by atomic force microscopy (AFM), Nanotec equipment, using a Nanosensors Si tip with a force constant of 40 N/m and a nominal radius of curvature <10 nm. The emission properties of the obtained nanostructures were measured at $T = 30$ K with a standard photoluminescence (PL) setup using a frequency-doubled Nd:YAG laser as excitation source (λexc = 532 nm, spot diameter ≈ 200 μm).

The experimental procedure starts growing a 0.5 μm thick undoped GaAs buffer layer at a growth rate rg = 0.5 monolayers per second (ML/s), As$_4$ beam equivalent pressure (BEP) of 2×10^{-6} Torr, and substrate temperature $T_s = 580$ °C on GaAs (001) substrates. The root-mean-square (rms) roughness of this surface is typically 0.24 nm. T_s is then decreased to 500 °C, and the nanohole template formation process is performed. It consists of a two-step process where metallic Ga droplets are first formed on the surface to be finally exposed to an As atmosphere. In particular, the growth protocol followed for the formation of Ga droplets consists of the opening of the Ga shutter during 20 s, with the cell providing a flux equivalent to the growth of GaAs at 0.5 ML/s. Simultaneously, the As cell is pulsed in cycles of 0.2 s open/0.8 s closed at a BEPAs$_4$ = 5×10^{-7} Torr. The result of this process is the formation of Ga droplets spread all over the surface with a density of 2×10^8 cm^{-2}. Finally, these Ga droplets are annealed under As atmosphere during 6 min at BEP$_{As4}$ = 5×10^{-7} Torr. About 30 s before the completion of the 6 min annealing period, the arsenic cell cracker is operated. This process ensures the production of an As$_2$ beam at the onset of InAs deposition. During this time, the substrate temperature is also increased to 510 °C. Before any InAs deposition, we observe that the surface presents randomly located nanoholes with an elongated structure along [110] direction and a density of 2×10^{-8} cm^{-2}. Their dimensions are $h = 4.4 \pm 0.7$ nm for the nanoholes depth and $D_1 = 43 \pm 3$ nm and $D_2 = 95 \pm 5$ nm for the nanoholes mean diameter along [1−10] and [110] directions, respectively. On this kind of patterned surface, 1.5 ML of InAs are deposited using two different As$_2$ pressures while keeping the rest of growth parameters constant. BEP As$_2$ used was 3.5×10^{-7} Torr and 1×10^{-6} Torr. InAs was deposited following a growth sequence consisting of 0.1 monolayers (ML) at a growth rate of 0.05 ML/s followed by a pause of 2s under the used As$_2$ flux. The substrate temperature is maintained during the

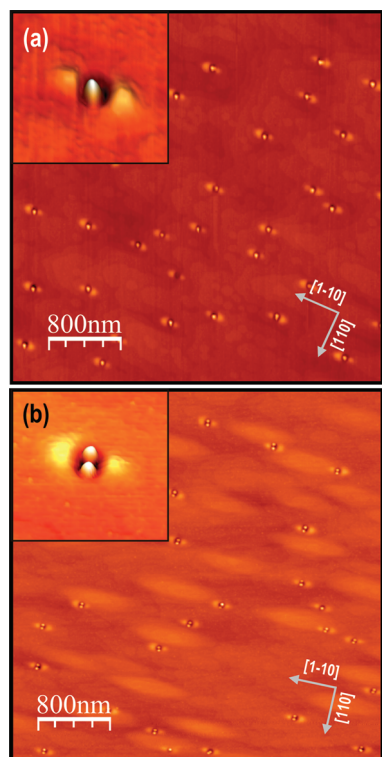* To whom correspondence should be addressed. E-mail: palonso@imm.cnm.csic.es.

Figure 1. (a) AFM image (4 μm $\times$ 4 μm) showing single quantum dots (QD) into GaAs nanoholes after growing 1.5 ML of InAs at BEPAs$_2$ = 3.5 $\times$ 10^{-7} Torr. The inset shows a detailed 3D image of a single QD. (b) AFM image (4 μm $\times$ 4 μm) showing QD pairs formed into GaAs nanoholes after growing 1.5 ML of InAs at BEPAs$_2$ = 1 $\times$ 10^{-6} Torr. The inset shows a detailed 3D image of a QD pair.

InAs deposition process at 510 °C. A (2 $\times$ 4) surface reconstruction was always observed during InAs deposition at the used As$_2$ pressures.

Once the InAs is deposited, a 100 nm thick capping layer is grown. It consists of an initial 20 nm GaAs layer grown at T_s = 510 °C under As$_2$ at BEPAs$_2$ = 1 $\times$ 10^{-6} Torr and a final 80 nm GaAs layer at conventional MBE GaAs growth conditions, T_s = 580 °C and BEPAs$_4$= 2 $\times$ 10^{-6} Torr.[16] Finally, on the top surface, the process for obtaining uncapped nanostructures on the nanoholes template is repeated for AFM topographic measurements.

Results and Discussion

Figure 1 shows AFM images corresponding to the deposition of 1.5 ML of InAs into the formed GaAs template at the two different As$_2$ pressures used in this work. Figure 1a shows the nucleation result when the lower As$_2$ pressure (BEPAs$_2$ = 3.5 $\times$ 10^{-7} Torr) is used during InAs deposition. It can be observed that a single QD is nucleated inside each of the nanoholes. The single QD occupancy is around 95%. In the inset of this figure a 0.5 μm $\times$ 0.5 μm 3D AFM image shows in detail one of these single QD. A different InAs nucleation behavior is observed in Figure 1b; in this case, by using the higher As$_2$ pressure (BEPAs$_2$ = 1 $\times$ 10^{-6} Torr) during InAs deposition, QD pairs aligned along [110] direction are formed inside each of the GaAs nanoholes. The double QD occupancy for this case is around 98% indicating a highly selective nucleation process at the nanoholes. The inset of this figure shows one of the QD pairs in a 0.5 μm $\times$ 0.5 μm 3D AFM image.

Figures 2(a−c) shows detailed 0.25 μm $\times$ 0.25 μm 3D AFM images for the initial nanohole, single QD, and QD pair structures, respectively. At their right, corresponding profiles along the [110] direction are also shown. The nanoholes, as already commented, are elongated structures along [110] direc-
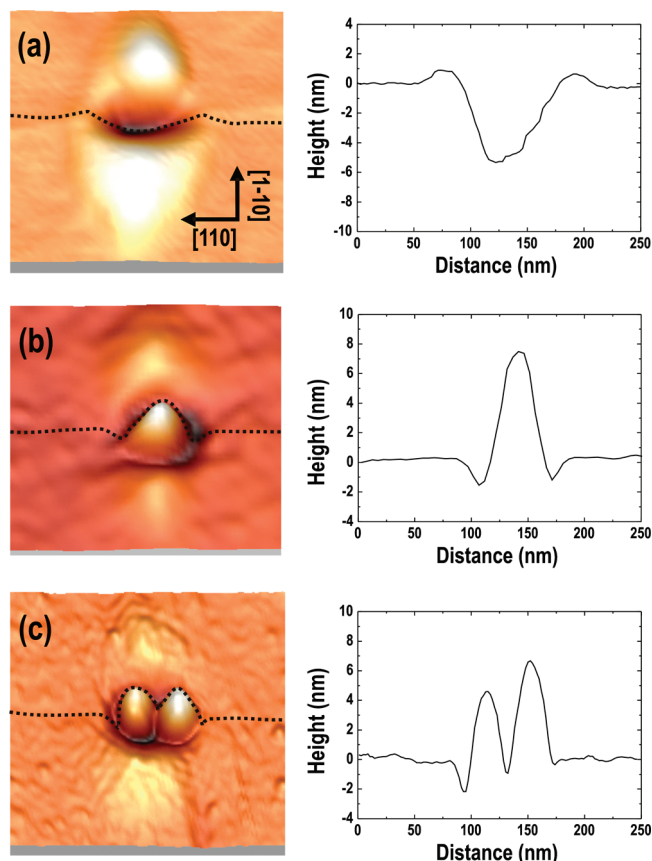

Figure 2. 3D AFM images (0.25 μm $\times$ 0.25 μm) corresponding to: (a) the initial GaAs nanohole, (b) single quantum dot occupancy at the nanohole, and (c) QD pair formation. Respective profiles of the nanoholes, single QD, and QD pairs are shown on the right.

tion with dimensions around 95nm in diameter along the [110] direction and 4.4 $\pm$ 0.7 nm in depth (Figure 2a). It has to be noticed that experiments reproducing the same growth conditions for the InAs nanostructures formation but without opening the In cell were performed and no significant differences in the dimensions of the nanoholes were observed.

Although AFM tip convolution effects at these small holes impede any possible facet identification inside them, it is expected, according to their orientation, that the lateral walls would be mainly B-type facets with steps along [110] direction.

In the case of single QD at the nanoholes (Figure 2b), these nanostructures show mean diameter of 58 $\pm$ 3 nm and height of 7.4 $\pm$ 0.8 nm, both quantities referred to the flat surface plane. In the case of QD pairs formation, systematic differences for QD heights are observed into the pairs, this effect permits to calculate two different height distributions, as represented by a two peaks Gaussian fit in Figure 3, with average values of 5.3 nm $\pm$ 17% and 6.6 nm $\pm$ 24%. It can be also observed in the QD pairs that the separation edge to edge between adjacent QD is practically zero within AFM resolution. A statistical mean value of 37 $\pm$ 4 nm is obtained for their diameter and peak to peak separation. According to previous reports on QD molecules[11] this QD peak interdistance is short enough to potentially observe quantum coupling phenomena. We want to notice that, as clearly observed in Figure 2b, single QD at the nanoholes are larger in size than those forming the pairs. However, we have observed that this size effect does not lead to a different PL peak energy (Figure 4). A similar QD PL energy emission in spite of size differences could be ascribed to a different In(Ga)As composition in the single QD and QD pairs. This
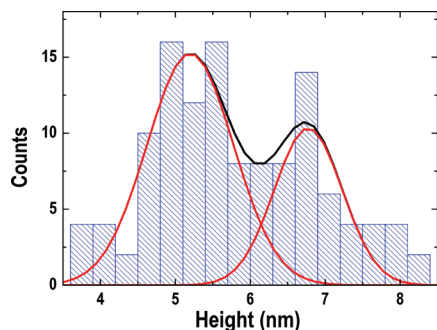
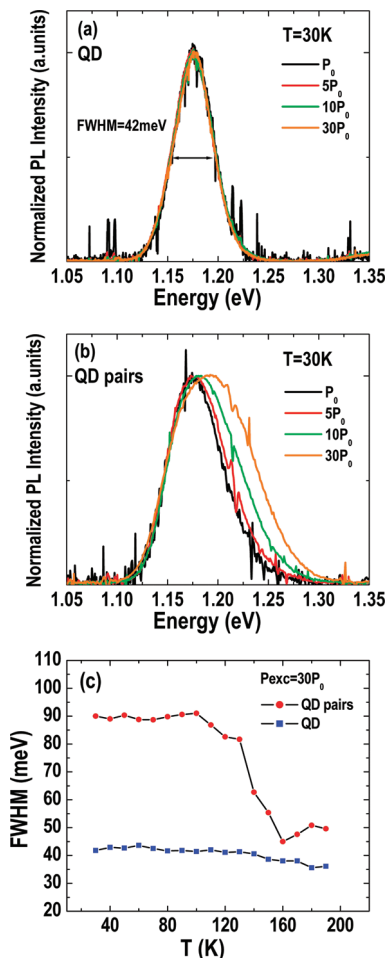**Figure 3.** Distribution of QD heights in the QD pair sample.

Figure 4. (a) Normalized single QD sample photoluminescence (PL) as a function of the excitation power. (b) Same for the QD pairs sample. (c) PL fwhm evolution as a function of temperature for QD pairs (red circles) and single QD (blue squares).

effect would be explained by a different Ga and In filling ratio at the nanoholes for the two different As_2 pressures used in this work. Thus, it seems that the role of arsenic pressure on the nucleation of either one or two QD inside otherwise identical nanoholes would be a change of Ga/In intermixing. According to previous works,[5,24] the change of reactivity of the different facets with arsenic pressure causes changes in the incorporation rates of the element III atoms. This effect would lead to the formation of QD with different composition and equilibrium size. The final result is then that for the same nanoholes profile, one QD (larger size, higher Ga content) or two QD (smaller size, lower Ga content) are nucleated at the nanoholes.

The normalized ground-state PL from the QD and the QD pairs as a function of the excitation power is shown in Figure 4a and b, respectively. The low excitation power used in these experiments ($P_0 = 0.03$ mW) avoids any emission from excited states as seen by the linear dependence of their integrated PL intensity (not shown).[22] The single QD sample luminescence, shown in Figure 4a, is characterized by a symmetric peak at 1.175 eV with a fwhm of 42 meV. Meanwhile, for paired nanostructures, shown in Figure 4b, the emission is centered at 1.18 eV with a broader fwhm of 63 meV. The similar PL energy observed for both kind of nanostructures independently of their distinct average size can be explained by their different In(Ga)As composition as commented above. In the single QD sample, a larger Ga content is necessary to push their energy levels upward and compensate their bigger average height. Increasing the excitation power, the luminescence of the QD pairs becomes asymmetric toward higher energies. In the same excitation range, no excited-state emission could be detected in the single QD sample which otherwise had a smaller number of QD per unit area. This fact has been related recently with the internal redistribution of carriers between the small and the large QD of each QD pair implying a certain degree of lateral coupling.[22,23] The participation of other resonant processes different from quantum tunneling in the ground state, as recently investigated by micro-PL studies of QD molecules, can not be concluded from our data.[11]

We observe also marked differences among the single QD and the QD pair samples investigating the temperature dependence of the PL fwhm shown in Figure 3c. Increasing the temperature, the single QD sample emission bandwidth remains almost constant in the studied range. Meanwhile, for the QD pairs, above 90K, the fwhm diminishes rapidly from its low temperature value (90 meV) up to ~50 meV at 200 K. It is well-known that thermally activated carrier redistribution from the QD toward the wetting layer can produce a reduction of the fwhm as the temperature is increased.[25] Given the shallower confinement of nanostructures emitting at 1.25 eV compared with typical QD, these phenomena can not be completely neglected in our case even at moderate temperatures. According to previous studies in similar systems, the differences found between both samples could also be related to carrier tunneling involving charge redistribution between the QD in the pairs.[22,23]

These PL results related to emission line shape dependence with excitation power and fwhm evolution with T can then be considered as preliminar signatures of lateral coupling in the QD pairs. However, to this respect, further optical studies at the individual QD pair level are mandatory to firmly establish the existence of QD molecules in this system.

Conclusions

In summary, we have studied the formation of low density In(Ga)As QD pairs laterally aligned along the [110] crystal direction. We have observed that the As pressure used during InAs deposition is a key parameter in order to control the formation of either single QD or QD pairs into previously in situ formed nanoholes. In particular, under the appropriate conditions we can obtain a 98% of double occupancy at the nanoholes. Our study of the ensemble emission of these QD pairs reveals spectral signatures usually associated to laterally coupled nanostructures which need to be confirmed by further investigation of their individual emission properties.

References

(1) Stevenson, R. M.; Young, R. J.; Atkinson, P.; Cooper, K.; Ritchie, D. A.; Shields, A. J. *Nature (London)* **2006**, *439*, 179.

(2) Hennessy, K.; Badolato, A.; Wigner, M.; Gerace, D.; Atatüre, M.; Gulde, S.; Fält, D.; Hu, E. L.; Imamoglu, A. *Nature (London)* **2007**, *445*, 896.

(3) Intallura, P. M.; Ward, M. B.; Karimov, O. Z.; Yuan, Z. L.; See, P.; Shields, A. J.; Atkinson, P.; Ritchie, D. A. *Appl. Phys. Lett.* **2007**, *91*, 161103.

(4) Heidemeyer, H.; Müller, C.; Schmidt, O. G. *J. Cryst. Growth* **2004**, *261*, 444.

(5) Songmuang, R.; Kiravittaya, S.; Schmidt, O. G. *Appl. Phys. Lett.* **2003**, *82*, 2892.

(6) Atkinson, P.; Ward, M. B.; Bremner, S. P.; Anderson, D.; Farrow, T.; Jones, G. A. C.; Shields, A. J.; Ritchie, D. A. *Jpn. J. Appl. Phys.* **2006**, *45*, 2519.

(7) Li, S. S.; Xia, J. B.; Yuan, Z. L.; Xu, Z. Y.; Ge, W.; Wang, X. R.; Wang, Y.; Wang, J.; Chang, L. L. *Phys. Rev. B* **1996**, *54*, 11575.

(8) Robledo, L.; Elzerman, J.; Jundt, G.; Atatüre, M.; Högele, A.; Fält, S.; Imamoglu, A. *Science* **2008**, *320*, 772.

(9) Stinaff, E. A.; Scheibner, M.; Bracker, A. S.; Ponomarev, I. V.; Korenev, V. L.; Ware, M. E.; Doty, M. F.; Reinecke, T. L.; Gammon, D. *Science* **2006**, *311*, 636.

(10) Beirne, G. J.; Hermannstädter, C.; Wang, L.; Rastelli, A.; Schmidt, O. G.; Michler, P. *Phys. Rev. Lett.* **2006**, *96*, 137401.

(11) Wang, L.; Rastelli, A.; Kiravittaya, S.; Atkinson, P.; Ding, F.; Bufon, C. C. B.; Hermannstädter, C.; Witzany, M.; Beirne, G. J.; Michler, P.; Schmidt, O. G. *N. J. Phys.* **2008**, *10*, 045010.

(12) Mano, T.; Watanabe, K.; Tsukamoto, S.; Fujioka, H.; Oshima, M.; Koguchi, N. *J. Cryst. Growth* **2000**, *209*, 504.

(13) Lee, J. H.; Wang, Zh. M.; Ware, M. E.; Wijesundara, K. C.; Garrido, M.; Stinaff, E. A.; Salamo, G. J. *Cryst. Growth Des.* **2008**, *8*, 1945–1951.

(14) Lee, J. H.; Wang, Zh. M.; Strom, N. W.; Mazur, Yu. I.; Salamo, G. J. *Appl. Phys. Lett.* **2006**, *89*, 202101.

(15) Wang, Zh. M.; Liang, B. L.; Sablon, K. A.; Salamo, G. J. *Appl. Phys. Lett.* **2007**, *90*, 113120.

(16) Alonso-González, P.; Fuster, D.; González, L.; Martín-Sánchez, J.; González, Y. *Appl. Phys. Lett.* **2008**, *93*, 183106.

(17) Liang, B. L.; Wang, Zh. M.; Wang, X. Y.; Lee, J. H.; Mazur, Y. I.; Shih, C. K.; Salamo, G. J. *ACS Nano* **2008**, *2*, 2219.

(18) Strom, N. W.; Wang, Zh. M.; Lee, J. H.; Abuwaar, Z. Y.; Mazur, Yu. I.; Salamo, G. J. *Nan. Res. Lett.* **2007**, *2*, 112.

(19) Alonso-González, P.; Alén, B.; Fuster, D.; González, Y.; González, L.; Martínez-Pastor, J. *Appl. Phys. Lett.* **2007**, *91*, 163104.

(20) Alonso-González, P.; González, L.; Fuster, D.; González, Y.; Taboada, A. G.; Ripalda, J. M.; Beltrán, A. M.; Sales, D. L.; Ben, T.; Molina, S. I. *Cryst. Growth Des.* **2009**, *9* (2), 1216.

(21) Li, S. S.; Xia, J. B. *Appl. Phys. Lett.* **2007**, *91*, 092119.

(22) Liang, B. L.; Wong, P. S.; Nuntawong, N.; Albrecht, A. R.; Tatebayashi, J.; Rotter, T. J.; Balakrishnan, G.; Huffaker, D. L. *Appl. Phys. Lett.* **2007**, *91*, 243106.

(23) Lippen, T. v.; Silov, A. Yu.; Nötzel, R. *Phys. Rev. B* **2007**, *75*, 115414.

(24) Shen, X. Q.; Kishimoto, D.; Nishinaga, T. *Jpn. J. Appl. Phys.* **1994**, *33*, 11.

(25) Sanguinetti, S.; Henini, M.; Grassi, M.; Capizzi, M.; Frigeri, P.; Franchi, S. *Phys. Rev. B* **1999**, *60*, 8276.